ELSEVIER

Polymer 41 (2000) 697–710

polymer

Low temperature cure of unsaturated polyester resins with thermoplastic additives
II. Structure formation and shrinkage control mechanism

W. Li, L.J. Lee*

Department of Chemical Engineering, The Ohio State University, 140 West 19th Avenue, Columbus, OH 43210-1180, USA

Received 31 December 1998; accepted 23 February 1999

Abstract

An important feature in the cure of unsaturated polyester (UP)/styrene/thermoplastics system is the formation of a two-phase structure. Its final morphology is primarily determined by the phase separation process and the gelation resulting from the polymerization. In this study, the phase separation process during the cure of UP resins with thermoplastic additives was investigated by optical microscopy. It was found that depending on the system miscibility and reaction kinetics, the formation of sample structure follows the same route, but may end at different stages with different types of structure. Two key factors—the volume fraction of the thermoplastic-rich phase and the phase separation period i.e. the time period between the onset of phase separation and the gelation—determine the final structure of the sample. Based on experimental results, a shrinkage control mechanism at low temperature cure was proposed.

Keywords: Unsaturated polyester resin; Phase separation; Shrinkage control

1. Introduction

The addition of thermoplastics as 'low profile' additives (LPA) to the unsaturated polyester (UP) resin can substantially reduce the shrinkage caused by the copolymerization between UP and styrene [1–2]. An important feature of the cure of UP/styrene/thermoplastics system is the formation of a two-phase structure (LPA-rich and UP-rich). This two-phase structure provides a weak interface where microcracking can initiate and microvoids can form, which in turn compensate the polymerization shrinkage. The final morphology is primarily determined by the phase separation process and the gelation initiated by the polymerization.

Phase separation is a common phenomenon in multicomponent polymeric systems due to incompatibility between the polymeric materials. Extensive experimental studies on phase separation have been carried out for thermoplastic polymer mixtures. The most frequently used experimental methods in studying phase separation in polymer mixtures are optical microscopy [3–5], time-resolved scattering techniques [4,6–8], and the pulse NMR method [4]. Theories about thermally induced phase separation in polymer blends have also been well developed. Depending on the depth of quenching, there are two types of distinguished phase separation: nucleation and growth (NG) and spinodal decomposition (SD). Nucleation and growth are associated with metastability. The NG mechanism results in dispersed domain size increasing with time, and the shape of the domains is spheroidal in nature. SD, however, occurs when the temperature is rapidly lowered into the spinodal region. In a phase separation by the SD mechanism, an interconnected cylinder-like structure (branch structure) tends to form during the early stage of phase separation. The branch structure tends to grow, coalesce and form larger spheroidal structure eventually. The late stage growth and coalescence is also called the 'coarsening' or 'ripening' process.

For initially miscible polymer blends, phase separation following the SD mechanism may create a three-dimensional co-continuous morphology (a high-level of phase interconnectivity for both the minor and the major phase). For initially immiscible blends, co-continuity can also be obtained near the phase inversion concentration without the aid of SD [9]. This is described as a nucleation, growth, and droplet coalescence mechanism by McMaster [10]. The formation of interconnected SD morphology of polymer blends via thermally induced phase separation has been addressed by many researchers [4,10,11]. Inoue et al.

* Corresponding author. Tel.: +1-614-292-6591; fax: +1-614-292-3769.

0032-3861/00/$ - see front matter
PII: S0032-3861(99)00178-0

[12,13] reported the development of the same type of structure in solution cast films of polymer blends. An example of a mechanically mixed polymer blend exhibiting co-continuous structure based on phase inversion is interpenetrating polymer blend [14–16]. The volume fraction ratio of the two components of these polymer blends is usually close to unity. Phase inversion mechanism is also applied to the toughening of the thermoplastics by the addition of rubber [17,18].

For spherical dispersions, the percolation threshold concentration for phase inversion, φ^C, is predicted to be 0.156 [19,20], which is found to be in reasonable accordance with experimental data [21]. Above the threshold, a more continuous disperse phase is obtained. Further increase in the fraction of the disperse phase will lead to phase inversion and a co-continuous structure. Phase inversion should occur between the range of φ^C and $(1-\varphi^C)$, suggesting that co-continuity can be formed within a range of composition rather than at a single point [22]. Several semi-empirical models for predicting phase continuity and phase inversion have been proposed [23–26]. The models are only valid for polymer blends formed by mechanical mixing (stirring and shearing).

The phase behavior in a reactive system is quite different from the thermally induced phase separation in thermoplastic polymer blends. In the latter case, phase separation takes place when system temperature changes from the one-phase region to the two-phase region, following either SD or NG mechanism. The boundary between the one-phase and two-phase region does not change. For a reactive system, the reaction results in changes of phase boundary and reactant composition. These changes force the system moving from the one-phase region to the two-phase region, and induce phase separation. There are only a few reports on the phase separation in reactive systems [27–30].

For a reactive system such as UP/styrene/thermoplastics, a detailed thermodynamic analysis is difficult because the reaction induced phase separation is an evolution process, with not only a change in composition but also an alternation of phase diagram. A conceptual model with phase diagram was proposed by Bucknall et al. [31] for the UP/styrene/PVAc reaction at high temperatures. However, little is known about the dynamics of phase separation in the formation of the microstructure. In this work, a study of the phase separation process during the cure of UP/styrene/thermoplastics system is presented. The effect of two important factors on the structure formation is addressed: the volume fraction of the LPA-rich phase and the competition between the phase separation and the gelation.

2. Experimental

The resins used in this study are Q6585 from Ashland Chemical (referred as Resin A) and Stypol 40-3961 from Cook Composites and Polymers (referred as Resin B). The properties of these resins have been described in Part I [32]. The thermoplastics chosen here are two poly (vinyl acetate), PVAc-A and PVAc-C, with molecular weight of 190,000 and 90,000, respectively, from Union Carbide, a saturated polyester (Q8000) and a polyurethane (LP8505) from Ashland Chemical. In all formulations, the ratio between the resin double bond and the styrene double bond was adjusted to 2.0 by adding extra styrene. An amount of 1.5% methyl ethyl ketone peroxide (Aldrich Chemical) and 0.5% cobalt octoate (Pfaltz & Bauer) were used as the low temperature initiator and promoter. All formulations contained 300 ppm benzoquinone as inhibitor.

The reaction kinetics was measured by a Differential Scanning Calorimeter, DSC (TA Instrument, MDSC 2910). Samples were sealed in aluminum sample pans which are able to withstand up to 2 atm internal pressure. Isothermal runs that ended with no further exotherm were followed by scanning the cured sample from room temperature to 250°C with a heating rate of 10°C/min, in order to determine the residual exotherm. The scanning run was then repeated to obtain the baseline. The measured heat flow data were then converted into conversion and reaction rate as a function of time, by assuming that thermophysical properties of the sample remained constant during reaction.

A Fourier Transform Infrared, FTIR, spectrometer (Nicolet, Magna-IR 550) with a resolution of 4 cm^{-1} in the transmission mode, equipped with a heating chamber, was employed to follow the conversion of styrene carbon–carbon double bond and unsaturated polyester carbon–carbon double bond during curing. The sampling interval was set at 2.5 min. Two absorption peaks were used to determine the concentration of the double bonds. The styrene C=C concentration is proportional to the absorption peak at 912 cm^{-1}, while the absorption at 982 cm^{-1} corresponds to polyester C=C. Since the peaks at 982 (polyester vinylene) and 992 cm^{-1} (styrene vinylene) overlapped, a subtraction method was used to separate the individual peaks [33].

A Rheometric Dynamic Analyzer (RDA) was used to evaluate the rheological changes that occur during the copolymerization of UP and styrene. Viscosity was measured under isothermal conditions and at a shear rate of 0.1 s^{-1}. The gel point is defined as the point where the reduced viscosity $\eta_r = \eta/\eta_0$ (η is the instantaneous viscosity and η_0 is the initial viscosity) reaches 10^3.

An optical microscope (Olympus, model BH-2) was employed to observe the phase separation process during curing. The optical microscope is equipped with a phase contrast attachment and an Olympus 35 mm camera (model PM-6). This device is capable of measuring the morphological changes when the size of the micro-structure is larger than 3 μm. A drop of resin mixture was bounded by two circular cover slips for observation. The microscope is also equipped with a heating chamber and a temperature controller.

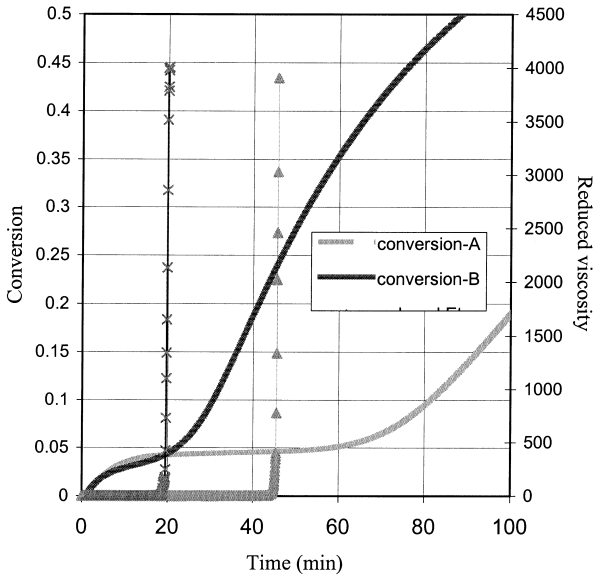

Fig. 1. Combination of conversion and viscosity profiles of the UP/St reaction of Resins A and B at 35°C.

3. Results and discussion

3.1. Cure behavior of resins A and B

The difference between Resins A and B on the cure behavior was studied. Fig. 1 combines the results of conversion profiles and viscosity profiles of the two resins cured at 35°C. It is clear that Resin B reacts much faster than Resin A at 35°C, and its final conversion is also much higher. The gel conversions of Resin B (i.e. 4.2%) was slightly lower than that of Resin A (4.6%).

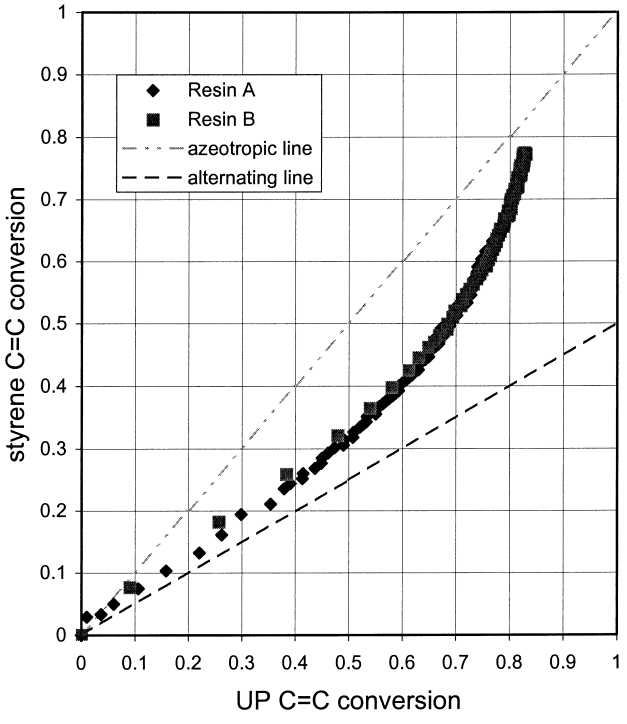

Fig. 2. The FTIR results of conversion of styrene carbon–carbon double bond versus the conversion of UP double bond of the two resins cured at 35°C.

The conversions of the styrene vinylene group versus the conversions of the UP vinylene group of the two resins obtained from FTIR are presented in Fig. 2. Both resins follow the same up-bending reaction route. The results clearly show that the copolymerization routes locate between the azeotropic and the alternating copolymerization line, and shift gradually toward the azeotropic line. At early stage, the polyester–styrene copolymerization is more favorable than the styrene–styrene homopolymerization due to the intra-molecular cyclization of polyester chains [33]. At high conversions, the styrene reaction becomes predominant as indicated by the up-bending curve, due to the low mobility of polyester molecules at high conversions. The overlapped reaction routes suggest a similar reaction mechanism of the two systems.

3.2. Phase separation study

The results in Part I [32] revealed that there were two transition points in both volume and morphological changes in the cure of UP/styrene systems/thermoplastics. Thermoplastics started to be effective on shrinkage control at the first transition point when the LPA-rich phase and the UP-rich phase became co-continuous. The shrinkage control effect vanished at the second transition point when the fusion among the particulate structure was severe.

Two factors strongly affect the way that the structure is constructed: the volume fraction of the two phases and the phase separation period, defined as the time period between the onset of phase separation and the macro gelation. To investigate the effect of the thermoplastic concentration on the volume fraction of the LPA-rich phase, we need to measure the volume fraction of each phase separately. This is difficult for the reactive systems because the volume fraction keeps changing during reaction. In the present work, a series of phase separation experiments were conducted by decreasing the temperature and forcing the phase separation to occur in samples without the presence of any curing agent. At room temperature, the mixture was clear and homogeneous. After storing at −2°C overnight, two distinct layers were found for most samples except the PU-containing ones. The upper layer was LPA-rich, and the lower layer was UP-rich [34]. Fig. 3 shows the volume fraction of the LPA-rich phase of several resin mixtures as a function of the thermoplastic concentration. It is interesting to note that the LPA-rich phase of the sample with 3.5% PVAc-A (the first transition point) has a volume fraction of 33%, while for the sample with 3.5% saturated polyester, the volume fraction of the LPA-rich phase is only 9%. Further increasing the amount of saturated polyester substantially increases the LPA-rich phase volume. At 9% saturated polyester level (the first transition point), the

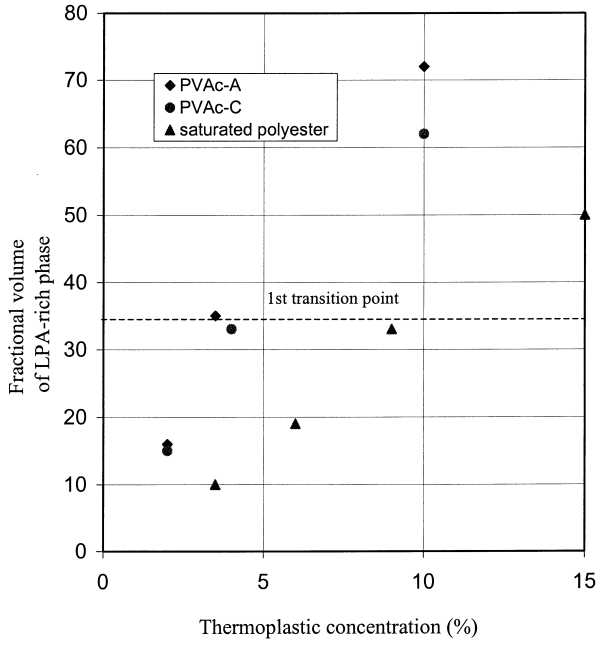

Fig. 3. Volume fraction of the LPA-rich phase versus thermoplastic concentration in Resin A when phase separation occurs at −2°C.

volume fraction of the LPA-rich phase reaches 33%. For all three thermoplastics, the first transition point occurs at a volume fraction of the LPA-rich phase around 33%. It implies that the percolation threshold, φ^C, is around this value under the test conditions. The difference on the thermoplastic concentration at the first transition for different thermoplastics (i.e. PVAc-A, PVAc-C, saturated polyester) can be attributed to their abilities in affiliating with the UP resin and styrene during phase separation. It should be noted that in the actual reaction, the volume fraction of the two phases may not be the same as the values reported here, but the trend should be the same.

The same method used for Resin A was also applied to Resin B to measure the volume fraction of the LPA-rich phase. However, even at −22°C, the samples containing 3.5, 4 and 6% PVAc-A remained homogeneous. The fact that Resin B is less likely to phase separate with temperature jump implies that Resin B systems are more compatible than Resin A systems.

For the UP/styrene/thermoplastics system, the driving force behind the phase changes is the copolymerization between UP and styrene. Therefore, the onset of gelation may also affect the structure formation through its competition with phase separation. It is reported that gelation stops phase separation and locks the structure [35]. The longer the time period from the onset of phase separation to the gel point, the more the phase separation can develop. The length of the phase separation period of the two resins was studied and compared. It is found that the onset of phase separation (t_p) and the gel point (t_g) of Resin B systems was much closer in comparison with that of Resin A systems. Fig. 4(a) and (b) show a comparison of t_p and t_g for the two

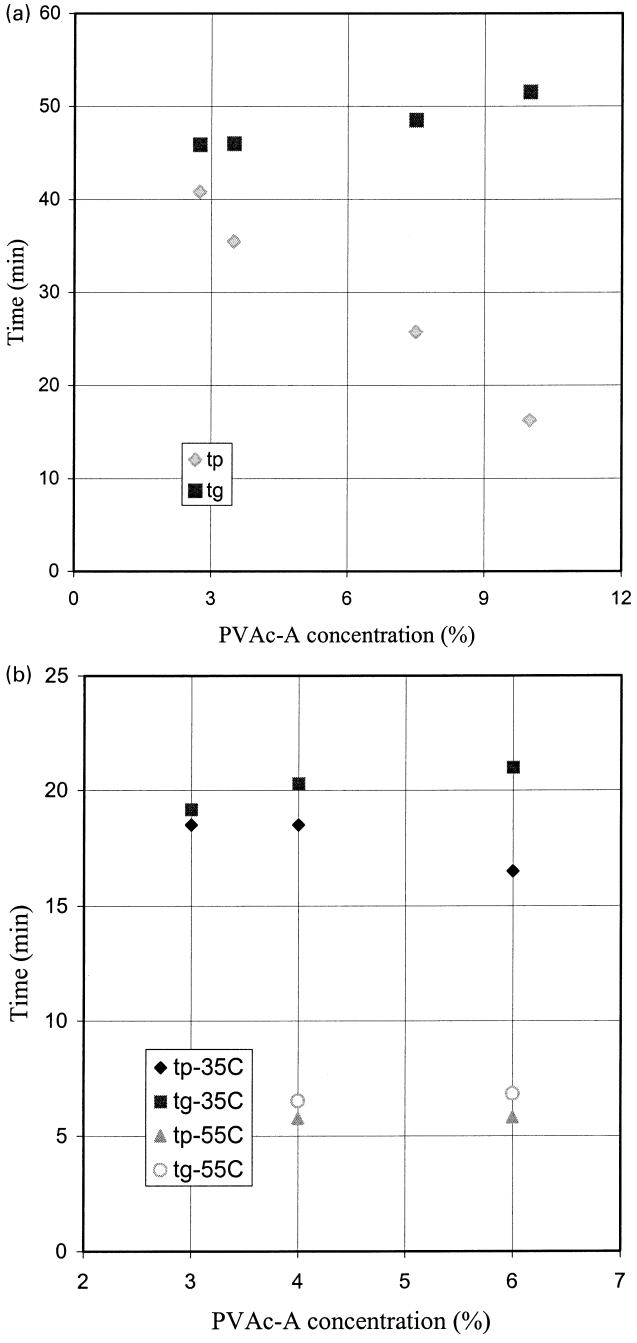

Fig. 4. The plot of the onset of phase separation and the gelation time versus PVAc-A concentration of: (a) Resin A measured at 35°C; and (b) Resin B measured at 35 and 55°C.

resin systems measured in a constant-temperature water bath (35°C). The onset of phase separation was noted by the onset of turbidity (cloudy point), while the gel point was determined when the resin stopped flowing. From these two figures, it is interesting to note that an increase in the amount of thermoplastics leads to an earlier phase separation but a prolonged gelation. In other words, the higher the thermoplastic concentration, the longer the phase separation period ($t_g - t_p$). Moreover, with the same

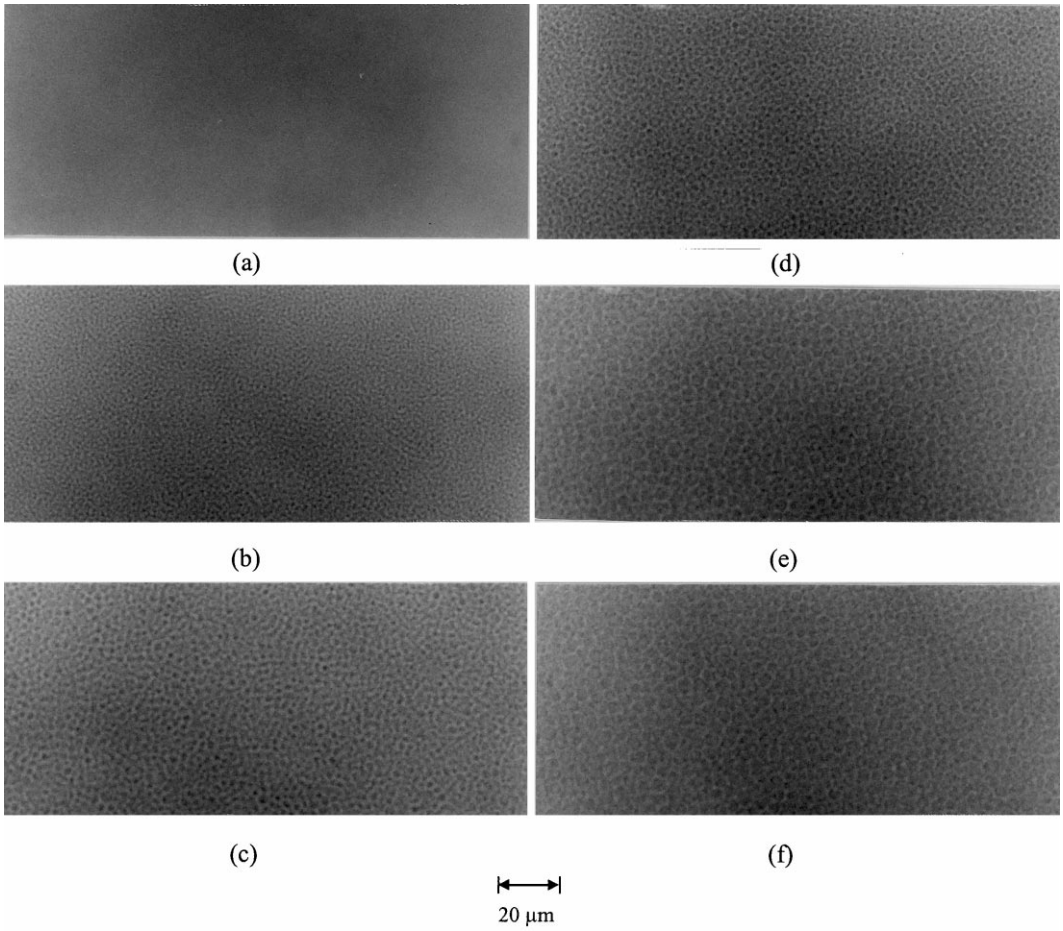

Fig. 5. Optical micrographs following the cure of Resin A with 8.5% saturated polyester (32°C). Gel time: 40.4 min. (a) 0 min; (b) 18.4 min; (c) 21 min; (d) 27.5 min; (e) 32 min; (f) 40.67 min.

thermoplastic concentration, the length of the phase separation period of Resin B systems is much shorter than that of Resin A systems. This indicates that macro gelation may affect the phase separation process of Resin B more than that of Resin A. At a higher temperature (i.e. 55°C), ($t_g - t_p$) becomes even shorter (Fig. 5(b)) due to a higher reaction rate.

Saturated polyester was chosen as the thermoplastic additive to analyze the dynamics of phase separation during curing using an optical microscope, because saturated polyester requires a higher concentration to be effective (refer to Part I). When the LPA-rich phase contains a higher percentage of thermoplastics, the phase contrast between the LPA-rich and UP-rich phase is higher and clear photos are easier to obtain. Three thermoplastic concentrations, 8.5, 9 and 11% were investigated. Among the three, 8.5% is just before and 11% is right after the first transition point (9%, refer to Part I [32]).

Fig. 5 depicts the phase separation process of the resin with 8.5% saturated polyester. The sample was initially homogeneous (Fig. 5(a)). At 18.4 min (Fig. 5(b)), spinodal decomposition took place with the formation of the interconnected structure (SD structure), indicating that the system went from the one-phase region rapidly to the unstable spinodal region. Coarsening and coalescence were observed in the late stage of phase separation (Fig. 5(c)–(e)), with the interconnected structure growing larger, breaking down and eventually coagulating into dispersed domains. Gelation occurred at about 32 min with a conversion less than 5% (Fig. 5(e)). The droplet-matrix morphology no longer changed after gelation (Fig. 5(f)).

The evolution of the phase separation process of the sample with 9% saturated polyester was significantly different from that with 8.5% saturated polyester. Fig. 6 shows the onset of SD phase separation appearing at 15 min (Fig. 6(b)), and the coarsening process proceeding rapidly within 2 min with the growth and breakdown of the interconnected structure (Fig. 6(b)–(d)). It suggests that the miscibility of this system decreased very fast and two distinct phases were formed. The dark area (the new phase, or the 'daughter' phase) is believed to be LPA-rich, while the light area (the old phase, or the 'mother' phase) is UP-rich. Further phase separation induced a clear change in phase structure between 16.5 and 17.33 min. Fig. 6(e) shows that the rapidly expanding LPA-rich phase encapsulated the initially continuous UP-rich phase and became a continuous matrix. In

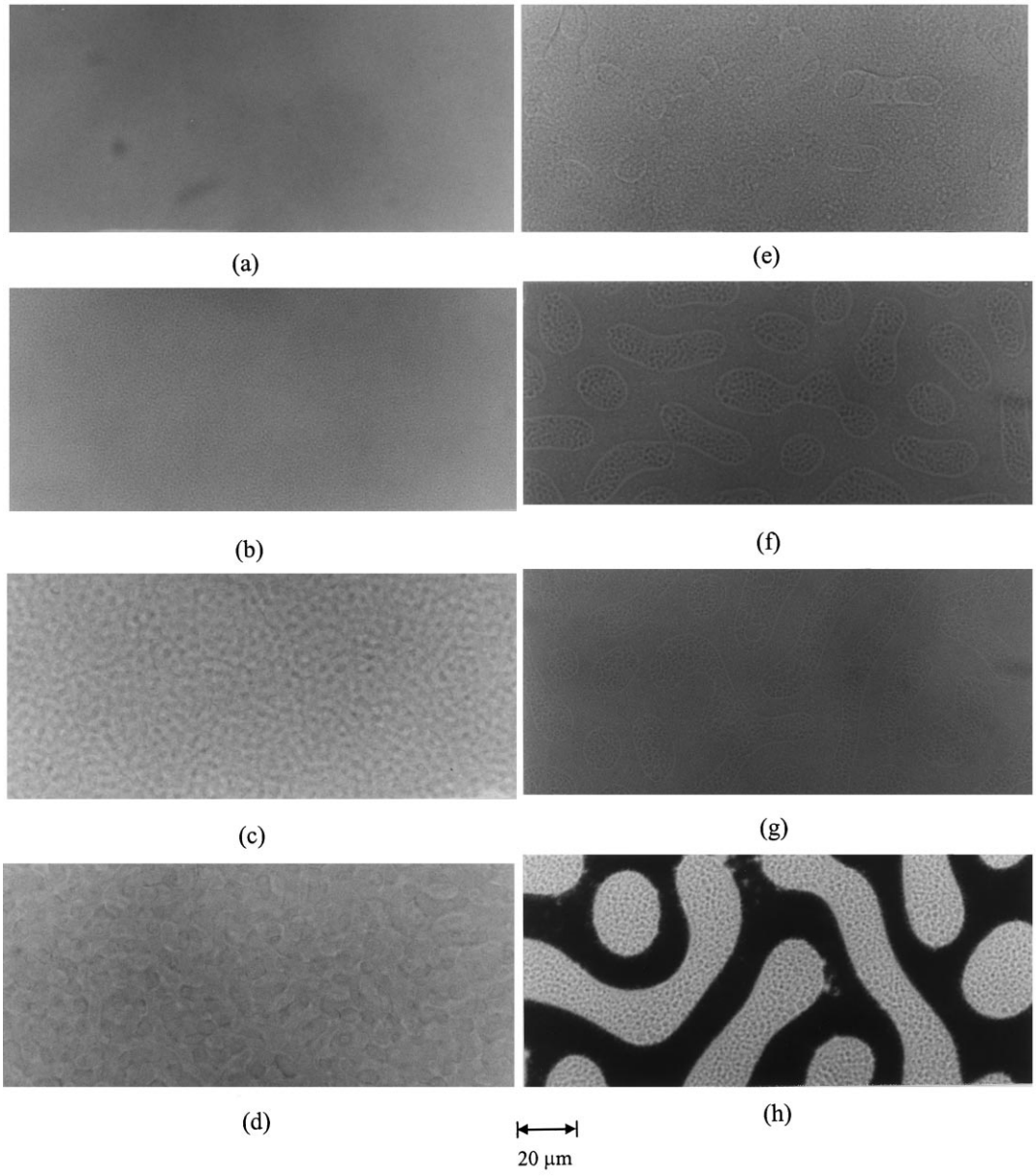

Fig. 6. Optical micrographs following the cure of Resin A with 9% saturated polyester (32°C). Gel time: 40.8 min. (a) 0 min; (b) 15.05 min; (c) 16 min; (d) 16.5 min; (e) 17.33 min; (f) 19.5 min; (g) 20.67 min; (h) >5 h.

Figs. 6(f)–(g), with the ongoing reaction, the entrapped UP-rich phase started growing, coalescing and eventually a co-continuous structure was formed at around 20.67 min. The increasing volume fraction of the UP-rich phase after coarsening can be attributed to the further polymerization in the LPA-rich phase, which forces the more reacting and the reacted UP to join the UP-rich phase. Gelation occurred between Fig. 6(g) and (h), and after that, the co-continuous structure remained unchanged with the reaction time. Microcracking was found only in the LPA-rich phase, as revealed by the final morphology in Fig. 6(h). Within both phases, much smaller particles or droplets (subinclusions) were detected due to the second level phase separation. This second level phase separation was gradually enhanced with the ongoing reaction.

Further increasing the saturated polyester concentration level to 11% (after the first transition point), the phase separation process followed the similar pattern as that with 9% saturated polyester (Fig. 7(a)–(f)). However, the onset of phase separation appeared earlier, and the UP-rich phase remained a dispersed phase. Again, microcracking was only observed in the LPA-rich phase.

Comparing the three series of micrographs, the increase of the volume fraction of the LPA-rich phase with the increasing thermoplastic concentration can be clearly identified. Microcracking was only found in the LPA-rich phase,

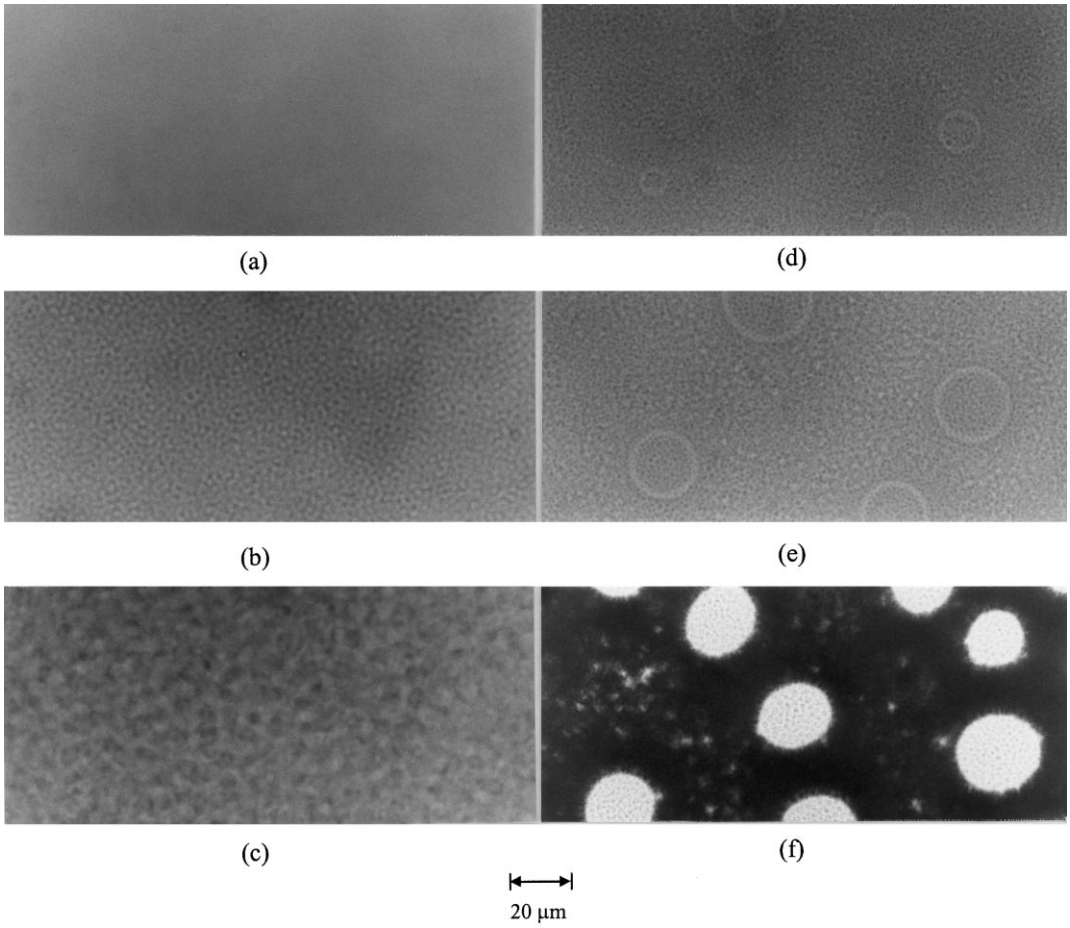

Fig. 7. Optical micrographs following the cure of Resin A with 11% saturated polyester (32°C). Gel time: 41.7 min. (a) 0 min; (b) 14.8 min; (c) 16 min; (d) 19.75 min; (e) 21.6 min; (f) >5 h.

and only when the LPA-rich phase became co-continuous or the continuous phase. The final morphology is in good agreement with the SEM photographs shown in Part I [32].

For the three samples studied, their phase separation process in the early stage is similar to that of the thermoplastic polymer blends. The evolution of phase structure of the sample with 8.5% saturated polyester (before the first transition) is virtually the same as that of thermoplastic polymer blends. However, the samples with 9 and 11% saturated polyester showed further structure evolution in the late stage of polymerization. In a typical SD of a thermoplastic polymer blend, one of the two interconnected structures would eventually break down and coagulate into a dispersed phase at the late stage of SD. For the sample with 8.5% of saturated polyester, the dispersed phase is the LPA-rich phase (i.e. the dark phase). While for the samples with 9 and 11% saturated polyester, the dispersed phase is the UP-rich phase (i.e. the bright phase). Apparently, the volume fraction of the two phases dictates the final morphology. The UP-rich phase may grow further due to polymerization in the LPA-rich phase. For the sample with 9% saturated polyester, this eventually leads to a co-continuous morphology with much larger scale. For the sample with 11% saturated polyester, the volume fraction of the LPA-rich phase is so large that it remains as the continuous phase through the entire reaction.

Summarizing the above results, it appears that the formation of the final sample structure initially follows the SD mechanism. The SD converts the system from a miscible to an immiscible mixture, and a fine SD type of co-continuous structure is formed. Further polymerization results in a change of the volume fractions of both phases, which leads to a coarsening stage. After that, the phase structure changes from a co-continuous structure to a droplet-matrix structure. When the volume fraction of the LPA-rich phase is low (i.e. lower than a value ϕ_{C1}), it will be the dispersed phase (e.g. 8% saturated polyester). The further increase of the UP-rich phase due to polymerization enhances the dominant role of the UP-rich phase, and the LPA-rich phase remains as the dispersed phase. However, when the volume fraction of the LPA-rich phase is high (i.e. greater than the value ϕ_{C1}), the UP-rich phase becomes the dispersed phase after coarsening. But the ongoing polymerization in both the LPA-rich and the UP-rich phase may lead to further development and coalescence in the UP-rich phase (e.g. 9 and 11% saturated polyester). The further growth of the UP-rich

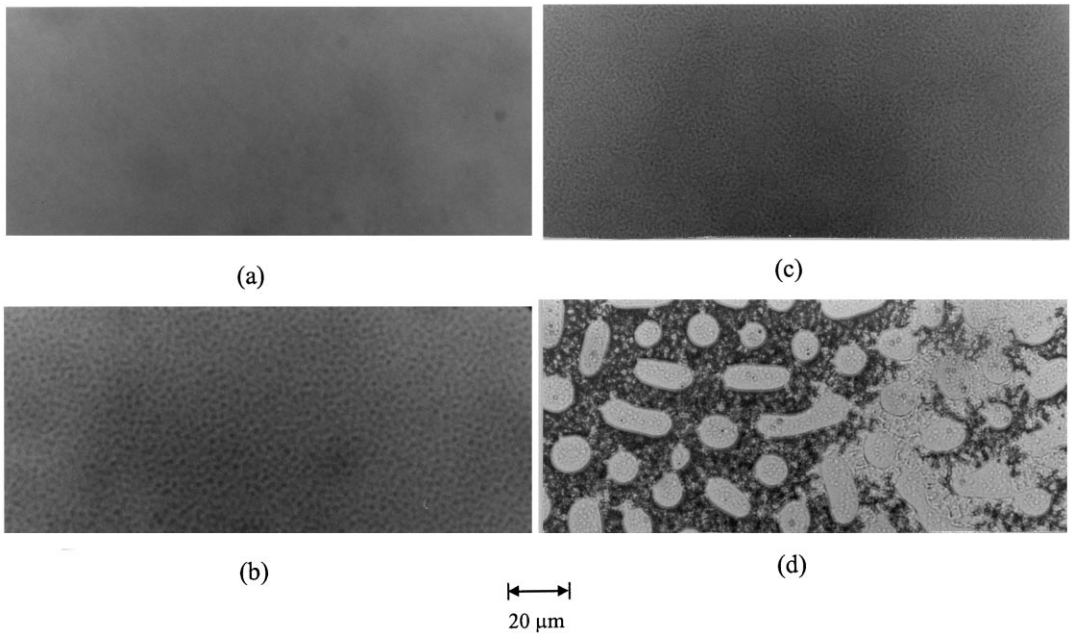

Fig. 8. Optical micrographs following the cure of Resin A with 3.5% PVAc-A (32°C). Gel time: 46 min. (a) 0 min; (b) 34.67 min; (c) 38 min; (d) >5 h.

phase may lead to two distinct structures: (a) when the volume fraction of the LPA-rich phase exceeds a value (ϕ_{C2}), the increase of the volume fraction of the UP-rich phase cannot reach the phase inversion composition, thus the UP-rich phase remains as the dispersed phase (i.e. 11% saturated polyester); (b) when the volume fraction of the LPA-rich phase is lower than ϕ_{C2} but higher than ϕ_{C1}, the growing UP-rich phase leads to a co-continuous structure again, but in a much coarse scale (i.e. 9% saturated polyester). In other words, between ϕ_{C1} and ϕ_{C2}, there is a range in which the system will form a co-continuous morphology. Outside this range, either the LPA-rich phase dominated or the UP-rich phase dominated droplet-matrix structure would form. Our experimental data showed that the sample with 10% saturated polyester had a similar co-continuous structure as the sample with 9% saturated polyester. The final shrinkage values of these two samples are also similar. The macro scale phase separation stops at the gel point, while the micro scale phase separation would continue locally. The latter can be considered as a secondary phase separation.

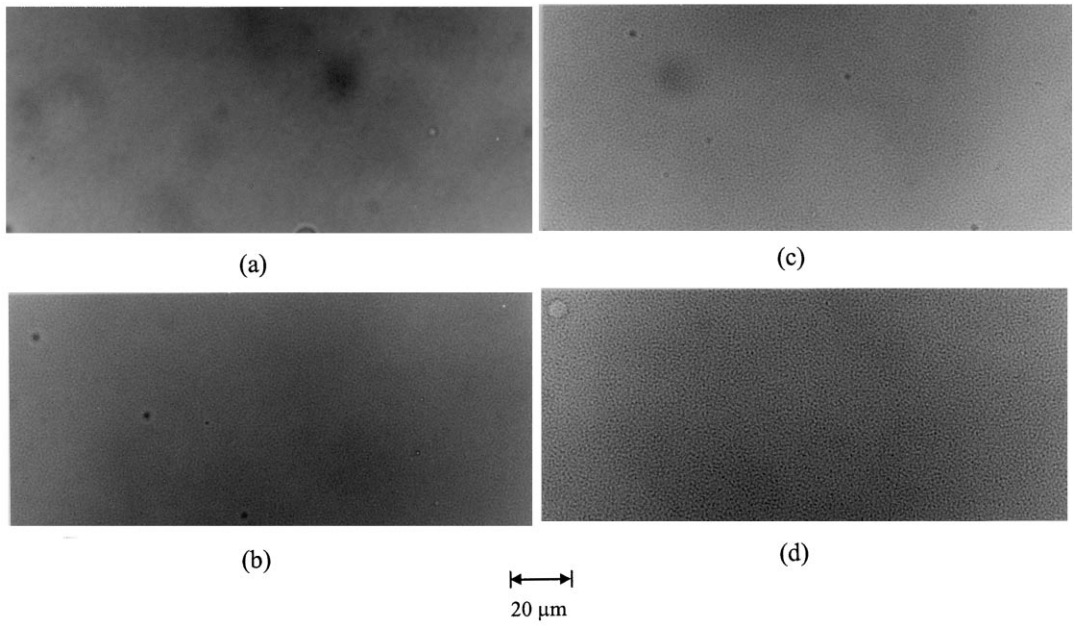

Fig. 9. Optical micrographs following the cure of Resin B with 3.5% PVAc-A (32°C). Gel time: 21.8 min. (a) 0 min; (b) 18.83 min; (c) 24 min; (d) >50 min.

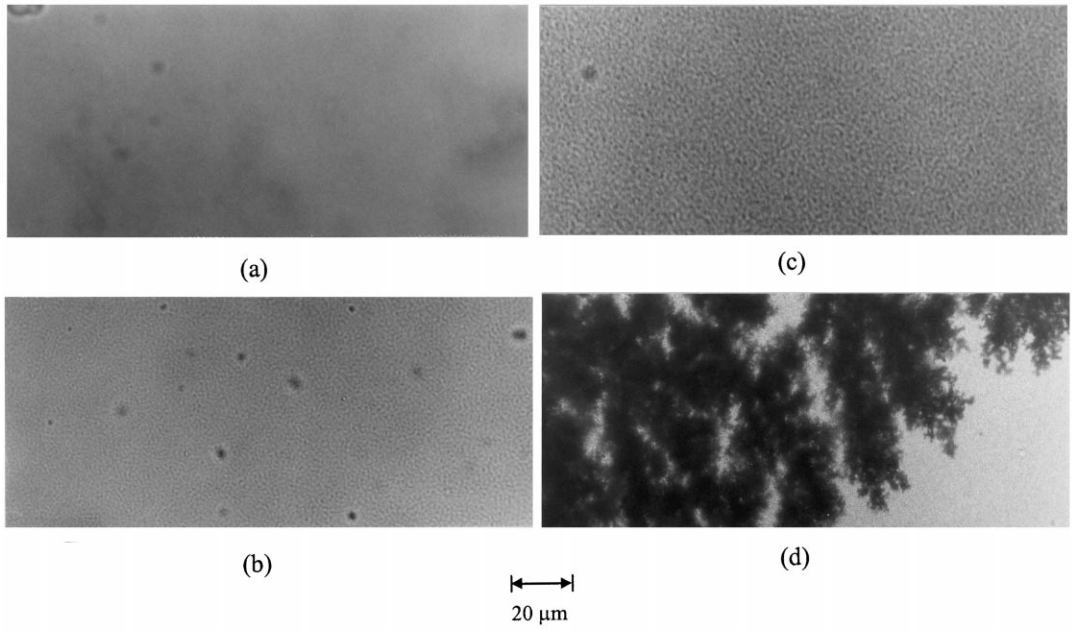

Fig. 10. Optical micrographs following the cure of Resin B with 6% PVAc-A (55°C). Gel time 6.0 min. (a) 0 min; (b) 3.83 min; (c) 6.09 min; (d) 30 min.

Comparison of the above mentioned phase separation to the volume-shrinkage–thermoplastic-concentration curves (refer Part I [32]) shows a good correlation. For all thermoplastics studied, there is a sudden drop of final shrinkage at the first transition. A slight increase of the thermoplastic concentration does not vary the shrinkage value significantly. However, if the thermoplastic concentration increases further, the shrinkage control efficiency gradually decreases. Combining the shrinkage-curve and the result of phase separation study, we can see that the first transition is a direct result of the formation of a coarse scale, co-continuous structure. This shrinkage control remains as long as the thermoplastic concentration still locates between ϕ_{C1} and ϕ_{C2}. The gradual increase of the final shrinkage when the thermoplastic concentration is larger than ϕ_{C2} is related to the gradual change of the structure from a co-continuous to an LPA-rich dominated structure. It is also noted that microcracking is always initiated at the interface between the LPA-rich and the UP-rich phase, and then propagated into the LPA-rich phase. The co-continuous structure provides the largest interfacial area for crack initiation, thus the best shrinkage control. The reason why the shrinkage control only occurs when the sample has a co-continuous or continuous LPA-rich phase will be discussed later.

From Fig. 6, we found that the time period from the onset of the phase separation to the completeness of the co-continuous structure was 5.6 min, while the time period from the onset of phase separation to gelation was 14.6 min. This indicates that gelation did not affect the macro scale phase changes. Thus, the volume fraction of the LPA-rich phase should be the governing factor which decides the final morphology in these systems.

A similar phase separation and inversion process was also observed in resin systems containing other thermoplastics. For example, micrographs in Fig. 8 illustrate the change of phase structure of the sample containing 3.5% PVAc-A. Its phase separation process is similar to that of the sample containing 11% saturated polyester. Again microcracking is initiated at the interface between the UP-rich and the LPA-rich phase, then propagates into the LPA-rich phase.

Fig. 9 depicts the change of phase structure during curing of Resin B with 3.5% PVAc-A at about 32°C. Fig. 9(a) shows an initially homogeneous system. The interconnected structure in Fig. 9(b) signifies the beginning of the SD at around 18.8 min. Fig. 9(c) (around 24 min) reveals slight coarsening due to the ongoing reaction. There is no difference between the final structure of this sample (Fig. 9(d)) and the one at gel point.

The phase separation process did not exhibit remarkable change when the thermoplastic concentration was increased to 6%. The only difference was that the coarsening in the late stage of phase separation was better developed. The breakdown of the SD structure created a few dispersed LPA-rich domains. Combined with its final morphology obtained from SEM in Part I, one can see that the increase in the thermoplastic concentration enhances the phase separation between the LPA-rich and the UP-rich phase, and tends to change the structure from branch-like to particulate-like. However, the LPA-rich phase remains as the dispersed phase and there is no microvoid formation.

Increasing the cure temperature to 55°C, the phase separation process remains the same as shown in Fig. 10 for Resin B with PVAc-A, except that the onset of phase separation is much earlier. It is interesting to note that the coarsening at a higher temperature is less developed in comparison with that at a lower temperature, probably

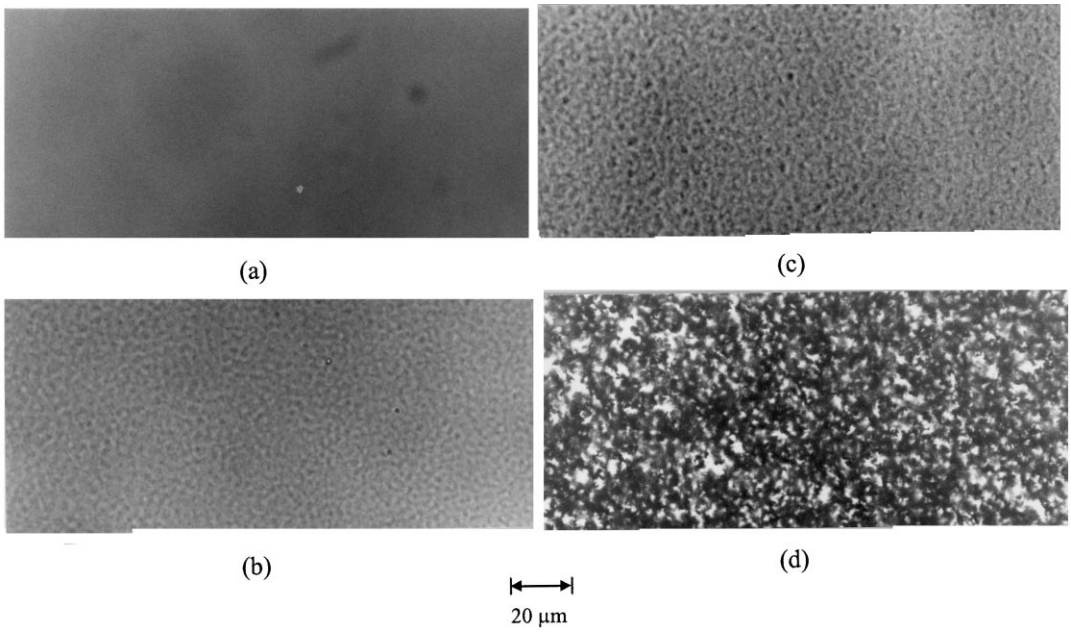

Fig. 11. Optical micrographs following the cure of Resin A with 9% saturated polyester at 55°C. (a) 0 min; (b) 4.25 min; (c) 16.5 min; (d) >5 h.

because of the shorter phase separation period. The dark, tree-branch-like structure, which appears at around 30 min suggests microcracking and microvoid formation in those regions. The structure change is similar when the same mixture was cured at 80°C.

The results of the optical microscopy study agree well with the SEM photographs shown in Part I [32]. At low temperatures, there is no microcracking, such that the fine co-continuous SD structure leads to a plain fracture surface in Resin B systems. At higher temperatures (i.e. 55 and 80°C), microcracking takes place at the interface of the fine co-continuous phases in the SD structure at low thermoplastic concentrations.

In comparison with Resin A systems, the final structure of Resin B systems was quite different. Unlike Resin A, the phase separation process would be locked at the SD stage by the macro gelation of the Resin B systems. The stress generated due to the polymerization at low temperatures is probably not sufficient to create microcracking and microvoids in such a structure.

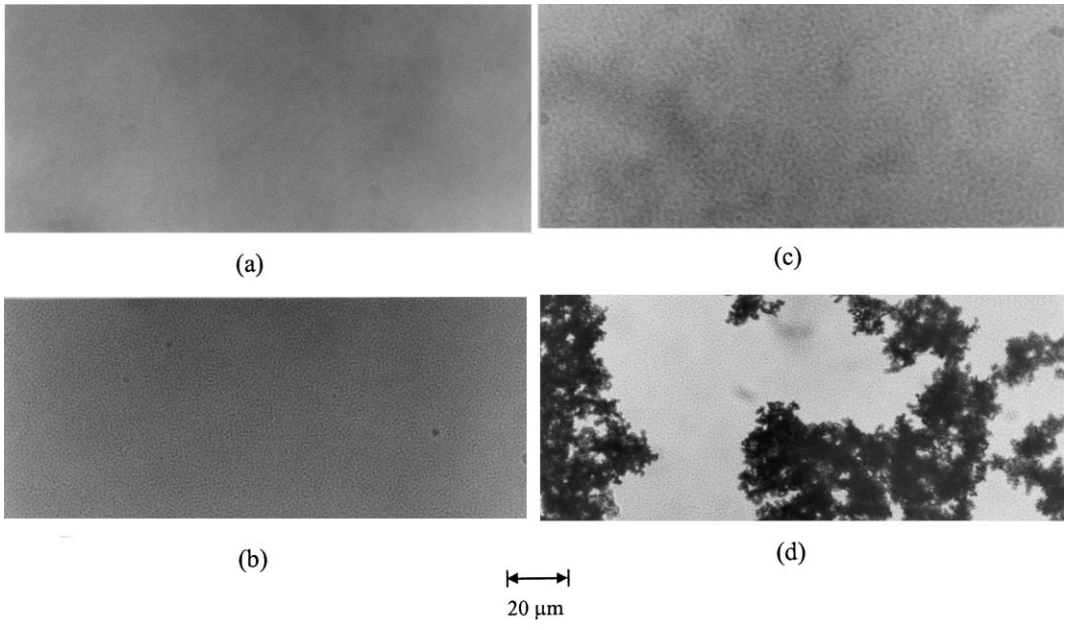

Fig. 12. Optical micrographs following the cure of Resin A with 9% saturated polyester at 80°C. (a) 0 min; (b) 2.51 min; (c) 5.51 min; (d) 6.75 min.

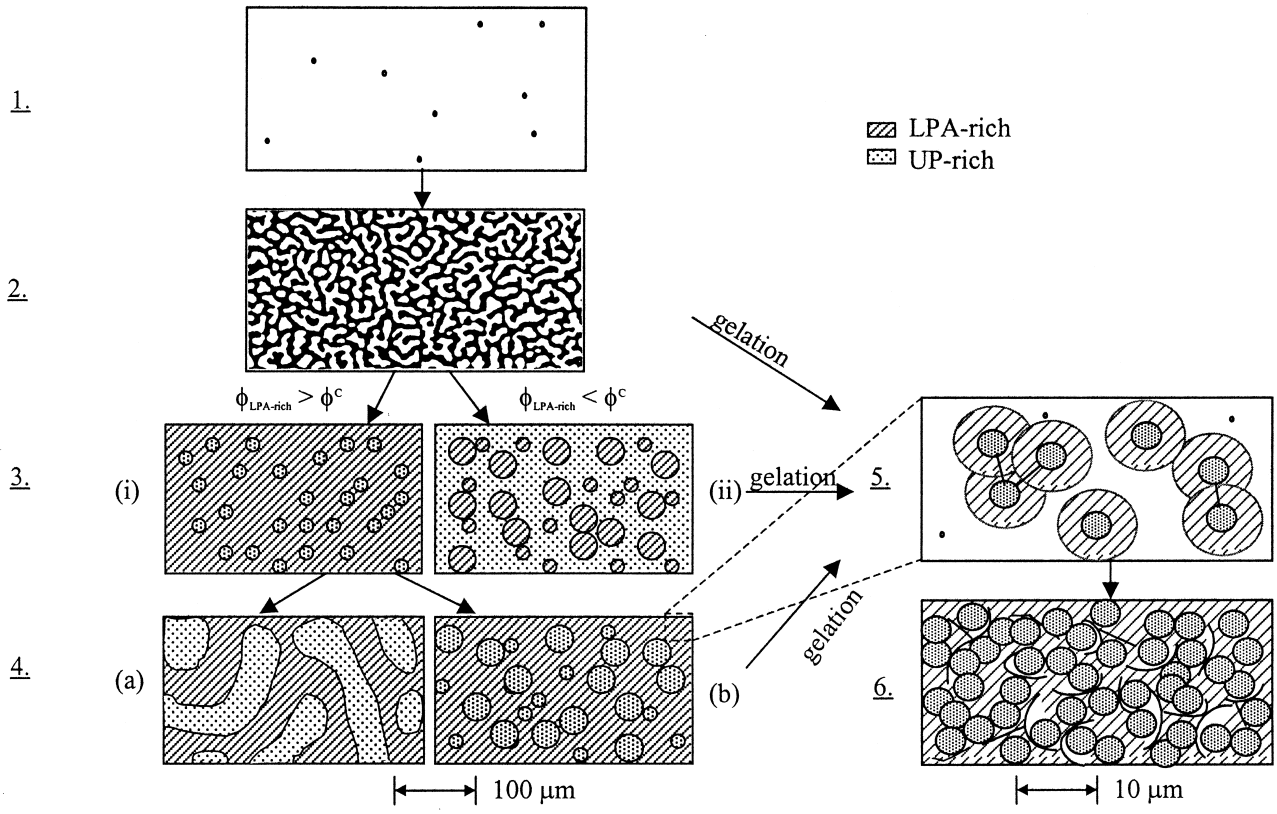

Fig. 13. Schematic of the shrinkage control mechanism at low temperature cure: (1) induction stage; (2) spinodal decomposition; (3) coarsening to (i) the LPA-rich phase dominated structure, or (ii) the UP-rich phase dominated structure; (4) coalescence and growth, (a) coarse co-continuous structure, or (b) LPA-rich phase dominated structure; (5) gelation; and (6) microvoid formation.

As demonstrated in the kinetic study, Resin B with 10.13 vinylene groups per molecule reacts much faster than Resin A, achieving a higher final conversion at the same reaction temperature. The backbone of Resin B contains isophthalic acid units. These units improve the compatibility of Resin B with styrene, and lead to a late phase separation. Early gelation and late phase separation are responsible for the SD type sample structure and poor shrinkage control of Resin B with PVAc-A at low temperature cure.

To further study the effect of the length of the phase separation period on structure formation, Resin A systems were cured at higher temperatures. Figs. 11 and 12 illustrate phase changes of Resin A with 9% saturated polyester cured at 55 and 80°C, respectively. It appears that unlike at 35°C, the phase separation was locked at the SD stage. Microcracking took place at the interface of the fine co-continuous SD structure.

3.3. Shrinkage control mechanism at low temperature cure

According to the results and discussion given in the previous section, we can divide the low temperature cure of the UP resins with thermoplastic additives into six steps, as illustrated in Fig. 13.

In Step 1, i.e. the induction period, the system starts as a homogeneous mixture consisting of UP, styrene, thermoplastic additive and initiator. This stage is caused by the presence of the inhibitor, which consumes the free radicals generated by the initiator. The propagation of the radical is suppressed by the inhibition effect [36].

In Step 2, the reaction starts when the inhibition effect is reduced to a low level. The UP molecules are linked by either inter- or intra-molecular reaction to form microgels. Because of the increase of UP molecular weight and the change of polarity, the compatibility of the reacting UP with surrounding thermoplastic and styrene decreases. This instability results in the occurrence of macro scale phase separation (i.e. primary phase separation), following the SD mechanism. An interconnected co-continuous structure is formed with an LPA-rich and a UP-rich phase. In this step, the system turns cloudy.

In the late stage of spinodal composition, coarsening and breaking down of the interconnected structure occur. Depending on the volume fractions of the two phases, two distinct droplet-matrix structures can be formed in Step 3. The volume fraction is decided by the characteristics of the thermoplastic and its concentration, the resin and the ongoing reaction.

In Step 4, with the continuous reaction and phase separation in both UP-rich and LPA-rich phase, the volume fraction of the UP-rich phase increases. If the sample morphology in Step 3 has a UP-rich continuous phase, the UP-rich phase

Table 1
Glass transition temperatures (T_g) of various thermoplastics measured by DSC at a scanning rate of 15°C/min

LPA	LPA-A	LPA-C	Saturated polyester	Polyurethane
T_g (°C)	33.2	29.23	~5	~−15

dominated structure would remain unchanged. If the sample morphology in Step 3 has an LPA-rich continuous phase, the LPA-rich phase dominated structure would evolve into one of the two types of structures: (a) a coarse co-continuous structure if the volume fraction of the UP-rich phase grows to the threshold of phase inversion; or (b) the same morphology where the UP-rich phase remains as the dispersed phase, but with larger domain size and higher volume fraction than in Step 3 because of its growth and coalescence.

In Step 5, the macro-gelation takes place and the structure formed through the primary phase separation is locked at this stage. Depending on the relative rate of polymerization and phase separation, macro-gelation may occur at Step 2, 3, or 4. After the gel point (the resin conversion is less than 5%), even though the primary structure is fixed, resin reaction and localized phase separation continue in the two primary phases to form the UP-rich particles surrounded by the LPA-rich layer. In Steps 2–5, the reaction mixture is cloudy and translucent. Resin viscosity starts to increase as the resin volume shrinks.

In the reaction, stresses may build up internally due to the polymerization shrinkage. At a certain point, i.e. Step 6, local cracking may occur along the interface of the two primary phases and propagate into the weaker phase (i.e. the LPA-rich phase). Microvoids are formed and stresses are partially released: consequently, the polymerization shrinkage is compensated. At this point, the reaction mixture turns opaque and volume expansion starts.

A quantitative analysis of microvoid formation during reaction is difficult. Conceptually, one can assume that microcracking would occur when the stress generated by the polymerization shrinkage is greater than the 'strength' possessed by the material at the interface or in the LPA-rich phase. The former depends on the copolymerization between UP and styrene, whereas the latter should be a function of the modulus of the material at the interface or in the LPA-rich phase, the stress relaxation behavior of the material, and the phase structure.

For the UP resin system cured at low temperatures, if there is no significant temperature variation, the polymerization shrinkage is the only driving force for microcracking. Polymerization shrinkage has been found to be proportional to the reaction conversion [37], thereby a function of cure time and temperature, as well as the reactivity of the system. Higher modulus solid is more crack-resistant, as suggested by the crack initiation criteria of the bulk material [38,39]. However, if a material stays in the liquid phase, it will not be able to bear any stress and therefore will not crack under stress. Ideally, for cracking to occur, the material should be a weak solid. Modulus is a function of resin conversion and the material properties. The viscoelastic deformation of a material can absorb energy through stress relaxation, which tends to prevent the growth of cracks. The relaxation behavior of the LPA-rich phase is a function of the physical property (i.e. T_g) of its major components. Table 1 lists the T_g of the four LPAs used in this study, measured by DSC at a scanning rate of 15°C/min. One can see that the glass transition temperatures of the two PVAcs are among the highest and the closest to the cure temperature. It implies that the stress relaxation of these two LPAs is lower than that of saturated polyester and PU. This is probably one of the reasons why PU is much less effective in compensating the polymerization shrinkage than PVAc at the first transition point [32]. It may also provide explanations as to why microcracking could not occur in some samples at the cure temperature (i.e. 35°C), but could occur when the cured sample was stored at room temperature (i.e. ~20°C). The driving and resistance forces for microcracking can therefore be expressed as:

Driving force (stress σ) = f{polymerization shrinkage[-f(resin conversion)]}
Resistance force = f{modulus[f(material properties, resin conversion)], stress relaxation[f(resin conversion, T_g)], phase structure[f(phase separation)]}

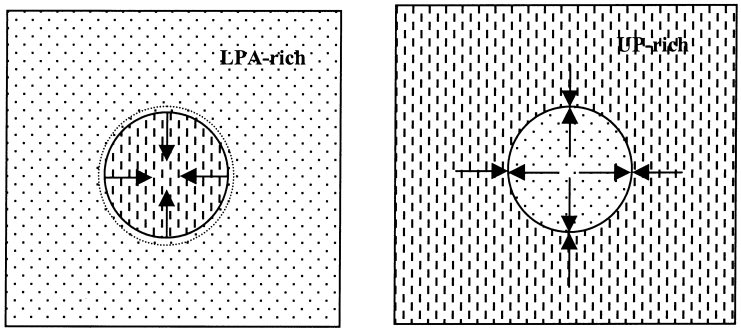

Fig. 14. Schematic of: (a) UP-rich phase dispersed in LPA-rich phase and (b) LPA-rich phase dispersed in UP-rich phase.

The type of phase structure is also critical to the microvoid formation. The SEM and optical micrographs show that microcracking occurs only when the LPA-rich phase becomes the continuous phase. A possible explanation is that if the UP-rich phase is the continuous phase, the shrinkage of the UP-rich phase would result in a contraction or compression on the dispersed LPA-rich phase, thereby concentrating the stresses on the interface and preventing microvoid formation inside the LPA-rich phase. However, when the UP-rich phase becomes the dispersed phase, shrinkage of the UP-rich phase would result in a tension force on the surrounding LPA-rich phase. This in turn would result in microcracking. Fig. 14 (a) and (b) shows the schematic diagrams of UP-rich phase dispersed in LPA-rich phase and LPA-rich phase dispersed in UP-rich phase morphology, respectively. These figures illustrate the possible mechanism of microcracking.

It is also noticed that changing the cure temperature does not vary the resin conversion at the volume expansion point. This suggests that at different cure temperatures, the driving forces (i.e. polymerization shrinkage) at the expansion point are similar. Therefore, the volume expansion observed at high temperatures is probably a result of the lower solid modulus at higher cure temperatures, which provides less resistance for crack initiation and propagation at the same resin conversion and the same sample morphology (i.e. small scale SD type of co-continuous structure). Other factors, such as a higher shrinkage rate at higher cure temperatures may also contribute to microcracking at high temperatures.

4. Conclusion

A co-continuous or LPA-rich phase dominated structure is essential for thermoplastics to be effective as shrinkage control additives at low temperature cure. In this article, the phase separation and the structure formation process of 'low profile' unsaturated polyester resin systems was studied by optical microscopy. It was found that, depending on the system miscibility and reaction kinetics, the formation of sample structure follows the same route, but may end at different stages with different types of structure. Two key factors, the volume fraction of the LPA-rich phase and the phase separation period, defined as the time period between the onset of phase separation and the gelation, determine the final structure of the sample.

Combining the dilatometry results with reaction kinetics and morphological and rheological data, a more complete understanding of the shrinkage control mechanism at low temperature cure is reached. Phase separation and microvoid formation are the two most critical steps for shrinkage control. Microcracking occurs when the stresses generated by polymerization shrinkage is greater than the 'resistance' force possessed by the interface or LPA-rich phase. This 'resistance' force must be related to the modulus of the material at the interfaces, or in the LPA-rich phase and stress relaxation behavior of the material. The detailed relationship, however, is still unclear.

Acknowledgements

The authors would like to thank Union Carbide, Ashland Chemical and Cook Composites and Polymers for material donation, and Ken Atkins and Rob Seats of Union Carbide for valuable discussions. Financial support of Union Carbide is greatly appreciated.

References

[1] Atkins KE. Low profile additives: shrinkage control mechanism and applications. In: Kia H, editor. Sheet molding compound materials: science and technology. New York: Henser, 1993.
[2] Melby EG, Castro JM. Comprehensive polymer science, vol. 7. Oxford: Pergamon Press, 1989.
[3] Smolders CA, van Aartsen JJ, Steenbergen A, Kolloid UZ. Polymer 1971;243:14.
[4] Nishi T, Wang TT, Kwei TK. Macromolecules 1975;8(2):227.
[5] Davis DD, Kwei TK. J Polym Sci Polym Phys Ed 1980;18:2337.
[6] Hashimoto T, Kumaki J, Kawai H. Macromolecules 1983;16:641.
[7] Hashimoto T, Sasaki J, Kawai H. Macromolecules 1984;17:2812.
[8] Han CC, Okada M, Muroga Y, Mccrackin FL, Bauer BJ, Tran-Cong Q. Polym Engng Sci 1986;26:3.
[9] Utracki LA. Polymer Alloys and Blends: Thermodynamics and Rheology. New York: Henser, 1989.
[10] McMaster LP. Advanced Chem Ser 1975;142:43.
[11] Nojima S, Tsutsumi K, Nose T. Polym J 1982;14:225.
[12] Inoue T, Kobayashi T, Hasimoto T, Tnaigami T, Miyasaka K. Polym Commun 1984;25:148.
[13] Inoue T, Ougizawa T, Yasuda O, Miyasaka K. Macromolecule 1985;18:57.
[14] Quintens D, Groeninckx G, Guest M, Aerts L. Polym Engng Sci 1990;30:1484.
[15] Andradi LN, Hellmann GP. Polym Engng Sci 1995;35:693.
[16] Mekhilef N, Favis B, Carreau PJ. J Polym Sci Part B: Polym Phys 1997;35:293.
[17] Wu W. Polymer 1983;24:43.
[18] Han CD, Chuang HK. J Appl Polym Sci 1985;30:2341 See also p. 2457.
[19] De Gennes PG. In: Goldman AM, Wolf SA, editors. Percolation localization and superconductivity, NATO ASI Series B, Physics, vol. 109. New York: Plenum Press, 1984. p. 83.
[20] Stauffer D. Introduction to percolation theory. London: Taylor and Francis, 1985.
[21] Lyngaae-Jorgensen J, Utracki LA. Macromol Chem Macromol Symp 1991;48/49:189.
[22] Ottino JM, Sax J. Polym Eng and Sci 1983;23(3):165.
[23] Paul DR, Barlow JW. J Macrmol Sci Rev Macromol Chem 1980;C18(1):109.
[24] Sperling LH. Interpenetrating polymer networks and related materials, ch. 2. New York: Plenum Press, 1981.
[25] Jordhamo GM, Manson JA, Sperling LH. Polym Eng Sci 1986;26:517.
[26] Miles IS, Zurek A. Polym Eng Sci 1988;28(12):796.
[27] Ludwico WA, Rosen SL. J Appl Polym Sci 1975;19:757.
[28] Verchere D, Sautereau H, Pascault JP, Moschiar SM, Riccardi CC, Williams RJ. Polymer 1989;30:107.
[29] Chou YC, Lee LJ. Polym Engng Sci 1994;34:1239.
[30] Hsu CP, Lee LJ. Polymer 1993;34(21):4497.

[31] Bucknall CB, Davies P, Partridge IK. Polymer 1985;26:108.
[32] Li W, Lee LJ. Polymer 2000;41:685.
[33] Yang YS. PhD thesis, The Ohio State University, 1988.
[34] Huang YJ, Su CC. J Appl Polym Sci 1995;55:305.
[35] Ruffier M, Merle G, Pascault JP. Polym Eng Sci 1993;33(8):466.
[36] Hsu CP, Lee LJ. Polymer 1993;34(21):4516.
[37] Muzumdar SV. Ph.D thesis, The Ohio State University, 1994.
[38] Griffith AA. Philos Trans R Soc 1921;A221:163.
[39] Orowan E. Phys Soc Rep Prog Phys 1948;12:186.